The National Facility Physics and Diagnostics

A. Wootton

August 6, 1999

DISCLAIMER

THE NATIONAL FACILITY PHYSICS AND DIAGNOSTICS

ALAN WOOTTON

Lawrence Livermore National Laboratory, P.O. Box 808, Livermore, CA 94550, USA

This paper presents a description of the National Ignition Facility, some of the physics experiments that will be performed on it, and a description of some of the diagnostics needed to complete these experiments. Experiments are presented under the headings of: ignition physics, weapons physics or high-energy-density experimental science, weapons effects, and basic science and inertial fusion energy. The diagnostics discussed are primarily those that will be provided for early operation.

1 Introduction

In January 1993 the then Secretary of Energy Admiral James Watkins approved the Justification of Mission Need for the National Ignition Facility (NIF), which authorized the conceptual design for the NIF. In December 1995 site-independent design funds were released by the then Secretary of Energy O'Leary. In December 1996, the Department of Energy (DOE) issued the Programmatic Environmental Impact Statement (PEIS) for Stockpile Stewardship and Management. This allowed DOE to proceed with the construction of the NIF, a $1.2-billion laser facility the size of a football stadium. The decision officially placed the NIF at Lawrence Livermore National Laboratory (LLNL), where it will be the latest in a series of high-power laser facilities used for research in inertial confinement fusion (ICF). The NIF design team includes experts from LLNL, Los Alamos National Laboratory, Sandia National Laboratory, the Naval Research Laboratory, and the University of Rochester's Laboratory for Laser Energetics. Official ground breaking occurred in May 1997, under the watch of the then Secretary of Energy Fredrico Pena. The target chamber, shown in Figures 1 and 4, was moved to its pedestal just after NIF day, May 1999, which was attended by the then Secretary of Energy Bill Richardson.

The NIF will play a major role in the Stockpile Stewardship Program (SSP), by allowing experiments in regimes relevant to nuclear weapons to be undertaken, regimes inaccessible by any other existing or proposed laboratory facilities.[1,2] Studies undertaken will contribute to data on materials under extreme conditions, information that can be used in developing and benchmarking advanced theoretical modeling tools, and testing aspects of particular weapons-performance issues. A key element of the stewardship program is the connection between the NIF and the Accelerated Strategic Computing Initiative (ASCI, a system of massively parallel

processors).[3] The NIF will attract scientists in fields that overlap weapons physics interests, and thus help maintain a cadre of scientists and technicians with weapons-relevant skills.

The main areas of investigation for the NIF are represented by four User Groups; ignition physics, weapons physics or high-energy-density experimental science, weapons effects, and basic science and inertial fusion energy. Accordingly this paper presents the physics program on the NIF under these headings. In addition, a Joint Central Diagnostics Team (JCDT) is responsible for proposing the target diagnostics, and those presently envisaged for early NIF operation are briefly described.

2   The National Ignition Facility

The NIF is scheduled for completion in 2003.[2,4,5] Figure 1 illustrates the building, approximately 550 ft. long and 360 ft. wide, with the U-shaped laser beam geometry leading to the 10 m internal diameter, 10 cm thick aluminum spherical target chamber. The target chamber is housed in a 30.5 m diameter by 29.3-m-tall, reinforced concrete building. The 192-beam, frequency-tripled ($\lambda = 0.35$ μm) Nd:glass laser system is designed with an on-target energy and power of 1.8 MJ and 500 TW, and can incorporate different beam-smoothing techniques.[6] Various pulse shapes with widths from ~1 ns to 21 ns will be available, with up to 3 full-system target shots per day. The 192 individual laser beams are directed into the chamber through 48 ports as 48 'quads'; each quad contains 4 individual beams. The quads are paired in "bundles" of two quads; each bundle consists of a quad directed to the upper hemisphere and a quad directed to the lower hemisphere. The laser is brought up in full bundles, i.e. in sets of 8 beams. The complete set of 24 bundles (48 quads, 192 beams) originate in 4 clusters, shown in Figure 1.

The chamber ports through which the laser quads enter have been chosen to accommodate both indirect x-ray drive and direct drive. Indirect x-ray drive utilizes a hohlraum to convert incident laser light to x-rays.[7] The design allows for multiple cones of laser light with different angles above and below the equator (23.5°, 30°, 44.5° and 50°), and for control of the laser light intensity between these cones during a shot. An example of the laser light angles is found Figure 2, where a cryogenic target is illustrated. Light from two of the quads that comprise two upper rings or cones are shown. All 48 quads are used to produce up-down or axial symmetry, 16-fold poloidal symmetry (i.e. 16 spots) in the outer cone of laser light, and 4-fold poloidal symmetry in the inner cone (i.e. 8 spots). The requirements for two cones of light with a power ratio, outer-to-inner, of 2:1, a minimum of 8-fold poloidal symmetry, and axial symmetry, dictate a

minimum or multiple of 48 beams. There is a practical maximum area for a single beam, ~1300 cm^2, which coupled with a maximum 3ω energy density of 9 J cm^{-2} (damage onset) allows a maximum energy per beam of about 11 kJ. This implies a minimum of 164 beams which, coupled with the symmetry requirements (multiple of 48), gives 192 beams. This number is also consistent with laser beam temporal smoothing using 4 different wavelengths per quad.[5]

1 of 4 clusters, each of 48 beams

Optics assembly
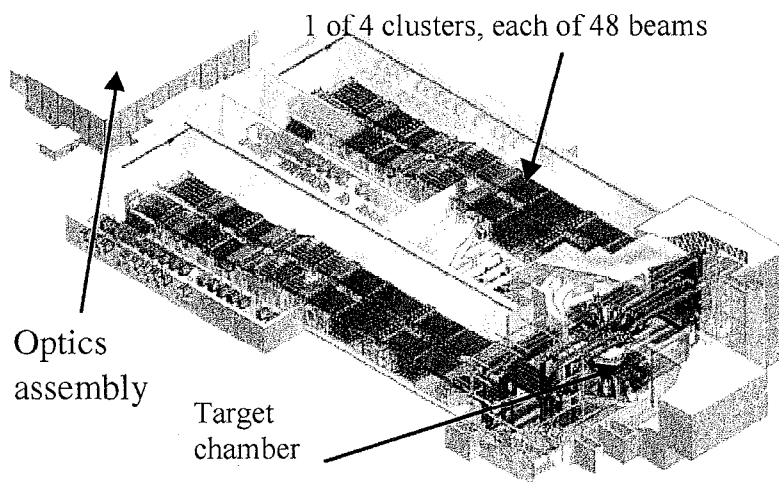
Target chamber

Fig. 1: The National Ignition Facility consists of a 192 beam frequency-tripled (λ = 035 μm) Nd:glass laser with an on-target energy and power of 1.8 MJ and 500 TW. The 192 beams are directed to the target chamber in 4 clusters of 12 quads, each quad consisting of 4 beams.

Laser beams

Heat-flow coupler

Cryostat

Cooling ring

Cryogenic fuel layer

Heater ring

Capsule ablator

Cooling ring

Heat-flow coupler

Fig. 2: A cryogenic hohlraum design, showing the cryogenic pellet, the surrounding hohlraum (He-H_2 filled) with cooling and heating rings, the cryostat and two incomimg laser beams for the upper hemisphere only. The design allows precise laser beam placement for implosion symmetry and accurate thermal control for cryogenic fuel layer uniformity. The hohlraum for this target is about 1 cm in length.

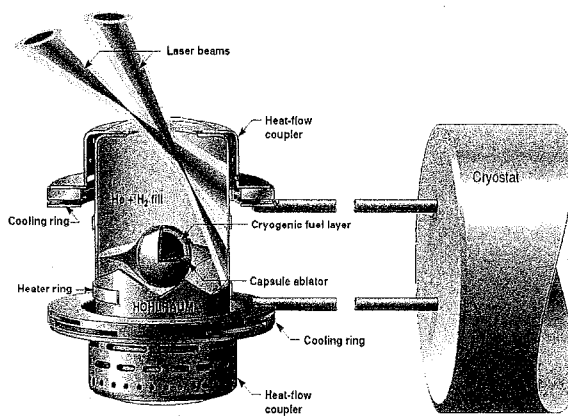One proposed start-up scenario, partially illustrated by Figure 3, is that initially a full cluster will be deployed (48 beams, one quarter of the NIF), including a single bundle dedicated to performance testing. This is shown by the plan view Figure 3a, illustrating both upper and lower hemisphere quads, and is the fastest way to maximize the available energy into a (horizontal) hohlraum, suitable for early high-energy-density experiments. Next, additional bundles will be added to allow symmetric illumination of a vertical hohlraum, suitable for the ignition campaign. Initially an outer ring of quads is added allowing 4-fold symmetry, followed by more outer quads (8-fold outer symmetry, Figure 3b). The next stage is to include inner quads (8-fold outer, 4-fold inner) allowing beam phasing (i.e. intensity control) between rings. Adding more outer beams allows back-lighting capability; inner and outer quads are then added to complete the installation (Figure 3c).
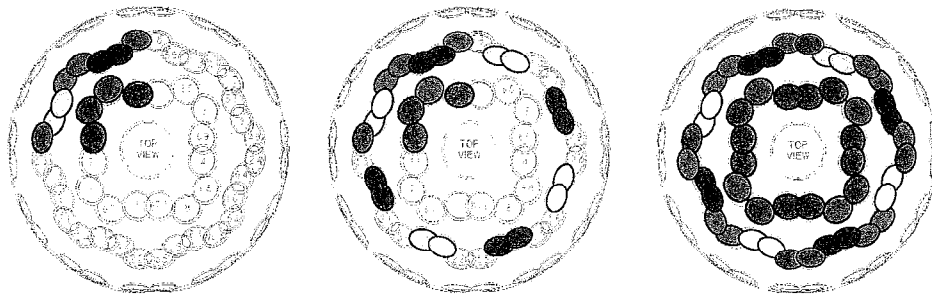

Fig. 3: A view from above the target chamber, showing left-to-right a possible sequence of beam activation. The projection shows quads directed through both upper and lower hemishere ports. Colors indicate the order in which quads are activated (after the first cluster the order is yellow, blue, gray, red, mauve, green) and the angles. The two quads in a bundle have the same color.

The three-dimensional geometry of "first light", a full cluster (48 beams) and half NIF (96 beams) is illustrated in Figures 4 and 5, in which some of the diagnostics to be deployed are also shown. Figure 4 shows a possible diagnostic set for first light, when the first bundle is activated. The diagnostics (see ref. 8 and references therein for a complete description) must characterize the laser beam pointing and spot size by monitoring the laser interaction with a simple disk or wedged target. One-dimensional (1-D) x-ray streak cameras (labeled SSC) and framing cameras (labeled TRXI) will resolve and synchronize to within ± 20 ps the x-ray emission from multiple laser spots focused at one time onto a target. Multiple snouts will be available later, allowing x-ray imaging with either pinholes or x-ray optics, and filtering with attenuation, x-ray mirrors or diffraction techniques (Bragg or Laue crystals). Where possible a diagnostic instrument manipulator, or DIM, will be used. These DIMs are two-stage telescoping systems that provide a mechanism for positioning of diagnostic packages, and enable exchange of manipulator

diagnostics between different institutions. The two static x-ray imaging diagnostics (SXI), that image the x-rays directly onto a CCD camera, will also monitor the beam pointing on test targets and on all target shots. Laser energy reflected from laser-produced plasmas in the form of stimulated Brillouin scattering (SBS) and stimulated Raman scattering (SRS) will be measured. A full aperture backscatter station (FABS) views the backscattered UV and visible light from the target that propagates back through the final focus lens and back down the beamline to the reflecting final turning mirror. The near backscatter imager (NBI) images part of the chamber wall, using cameras to separately measure the SBS (near 351 nm) and SRS (400-700 nm) scattered light.
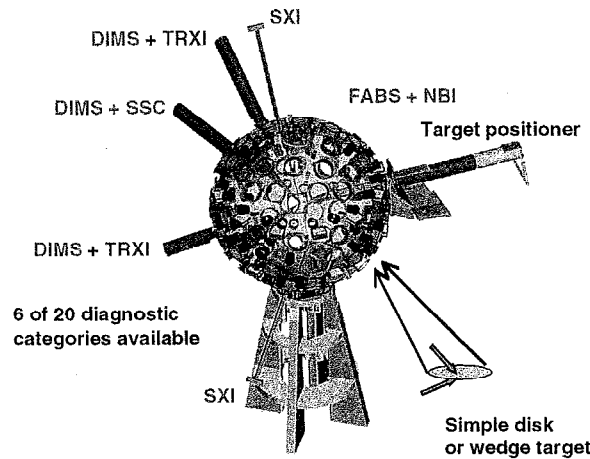

Fig 4: A possible early configuration, with one bundle (two quads) shown illuminating a simple disk target as might be used for laser spot size and pointing verification.
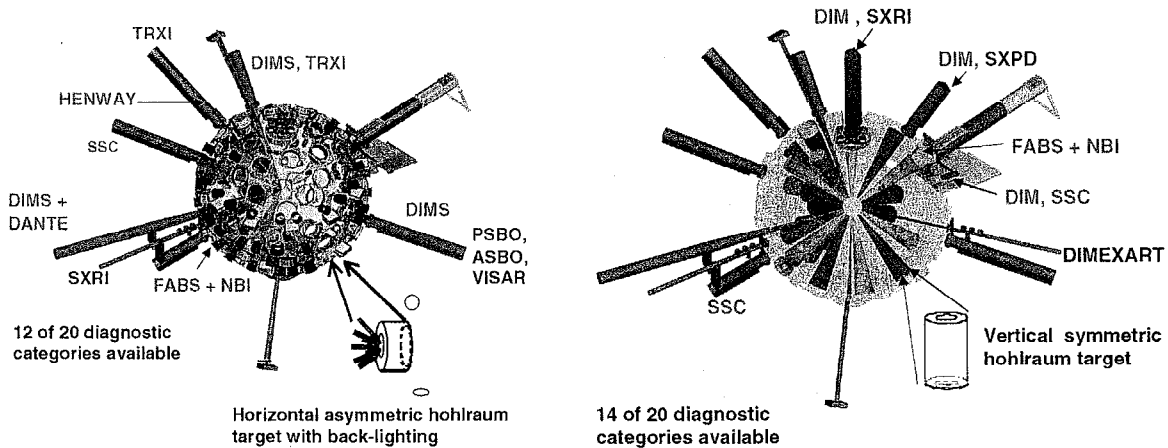

Fig 5: Views showing a possible diagnostic deployment when a) a full cluster is used to illuminate an asymmetric horizontal hohlraum, and b) symmetric illumination of a vertical hohlraum is available.

When the first cluster is deployed, as shown in Figure 5a, the available diagnostics must be capable of measuring hohlraum drive temperature, and shock velocities. With symmetric illumination available the diagnostics must be moved (Figure 5b). The soft x-ray power diagnostic (SXPD) measures the x-ray emission from a hohlraum through a lined hole in its wall or through the laser entrance hole, giving the time history of the radiation temperature inside the hohlraum. It uses a transmissive diffraction grating to disperse the x-ray flux onto an array of Si photodiode detectors. The Dante is the traditional diagnostic for this purpose, based on calibrated x-ray filters, mirrors, and vacuum x-ray diodes. A DIM-based system (DIMEXART) based on x-ray diodes is being develop by the French. The primary mission of the soft x-ray imaging diagnostic (SXRI) is to measure the time-dependent size of the soft x-ray diagnostic hole in hohlraums. As a secondary mission, it will also be used to study the spatial symmetry of the radiation drive in these hohlraums. The shock breakout systems measure velocities of e.g. shocked packages attached to hohlraums. The passive shock breakout system (PSBO) monitors the visible emission that occurs when a shock breaks out from a stepped or wedged witness plate; the time difference across known distances provide the velocity. The active shock breakout system (ASBO) augments the temperature range of the PSBO using a laser to probe the back surface of the diagnostic witness plate; when the shock wave reaches the back surface of the witness plate, it rapidly heats the surface, causing the reflectivity to drop dramatically. A velocity interferometer system (labeled VISAR) is also planned. Finally neutron diagnostics arc required for the start of the ignition experiments using D-T (in 2007). The core target diagnostic set provides a time-of-flight measurement of ion temperature, a total yield from sample activation, and will transfer a neutron spectrometer previously used on Nova.
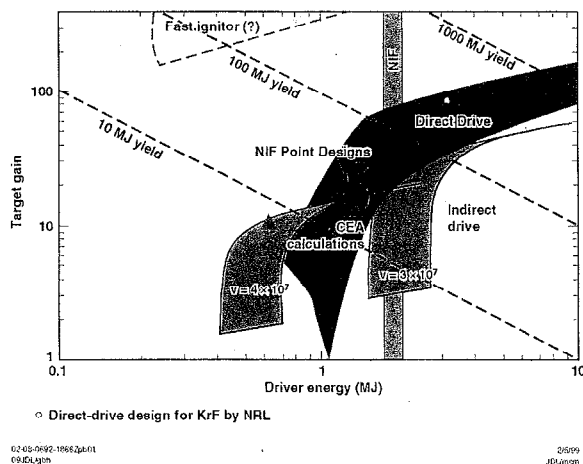
3 Ignition physics

Fig. 6: The NIF ignition thresholds and regions of the gain curve for multiple target concepts.

The NIF will map out the ignition thresholds and regions of the gain curve for multiple target concepts. Predictions are shown in Figure 6 for indirect drive, direct drive, and a possible fast ignitor scenario.[7] The NIF point design is for a 1.3 MJ pulse, although 1.8 MJ is available (3ω).

In inertial confinement, burn of an ignited fuel mass typically is quenched by hydrodynamic expansion. Details can be found in reference 7 and references therein. From the outside of the fuel, a rarefaction wave moves inward at the speed of sound, C_S. By the time this rarefaction has moved a fraction of the radius r, the fuel density in most of the fuel mass has dropped significantly, and the fuel no longer burns efficiently. Because of this, the confinement time is proportional to the compressed fuel radius r.

$$\phi = \frac{\rho r}{\rho r + 6(g/cm^2)} \approx \frac{N_0 \tau}{N_0 \tau + 3 \times 10^{15}(s/cm^3)} \quad ,$$

Here ϕ is the fuel burn-up fraction, τ is the confinement time, N_0 is the particle number density, and ρ is the matter density in the fuel. Both direct drive and indirect drive targets rely on central ignition followed by propagation of the burn via alpha deposition and electron conduction into a surrounding colder fuel. Once the hot central region of the fuel reaches 10 keV with a product ρr equal to the range of the alpha particles (~0.3 g/cm^2 at 10 keV), the burn will propagate into and ignite an indefinite amount of surrounding cold fuel. To achieve the hot-spot ignition conditions requires an implosion velocity ~4×10^7 cm/s. The gain is given by

$$G = \phi E_{fusion} \frac{M_{fuel} + M_{hot-spot}}{E_{hot-spot} M_{hot-spot} + \alpha 3 \times 10^5 \rho^{2/3} M_{fuel}}$$

where the specific energies are

$$E_{fusion} \approx 3 \times 10^{11} J / gm; \quad E_{hot-spot} \approx 1 \times 10^9 J / gm \ (at \ 10 keV);$$

$$E_{fuel} \approx \alpha 3 \times 10^5 \rho^{2/3} J / gm; \quad \alpha = \frac{P_{fuel}}{P_{Fermi}}$$

The highest gains are achieved by minimizing α, i.e. keeping the compressed fuel as cold as possible. Fuel compression with minimal heating is provided by a carefully tailored laser light intensity history, and thus a specific ablation and pressure history.

The physics involved in achieving ignition can be categorized under five headings: 1) hohlraum energetics (laser pulse shape and pointing, laser beam profile and smoothing, hohlraum design), 2) drive symmetry (effects of hohlraum plasma on beam propagation, hohlraum wall

motion, laser beam phasing), 3) capsule physics (ablation rate, implosion velocity, shock timing, implosion stability), and 4) ignition implosions (capsule design and fabrication, cryogenic systems, tritium fill, ignition diagnostics). A series of experiments on the Nova facility, presently being augmented by experiments on Omega, has demonstrated that the physics is understood.

Yield vs capsule microroughness (σ_{out})

$$\frac{\text{Yield}}{\text{Clean 1D yield}}$$

$C_r = 12$

- Nova data
- 3D Simulations

σ_{out} (m) rms

NIF surface finish

(3D simulations include ℓ = 2, 4, 6, and estimates of m = 5 perturbations)
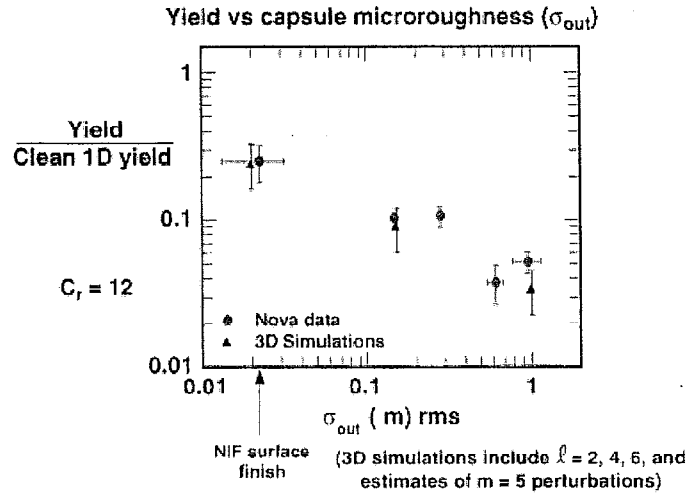
Fig. 7: A comparison of experimental neutron yield on Nova with 1-D (without surface roughness) and 3-D (with surface roughness) predictions, showing the data is understood.

Not only can the individual components required to achieve ignition be understood, but also integrated D-T implosions themselves: for example the neutron yields for high growth-factor implosions on Nova agree with three dimensional modeling that includes all sources of asymmetry. Figure 7 shows results where the neutron yield was measured as a function of surface roughness, and compared both to 3-D predictions that included the roughness, and 1-D predictions that ignored the roughness.[9] Clearly surface finish is crucially important, because of the mixing caused by hydrodynamic instabilities driven during the implosions. This situation (of well-understood physics) is different from that found in magnetic fusion, where the physics of e.g. electron confinement remains to be understood. The experimental challenge of inertial confinement ignition in the laboratory is to simultaneously achieve conditions only achieved independently to date.

4   High-energy-density physics

With the advent of megajoule class lasers, focused into mm-scale volumes, access to the very high-energy-density-regimes only previously attainable by nuclear testing and in some

astrophysical situations will be available. Three main experimental areas of focus will be equations of state (EOS), hydrodynamic instabilities, and radiation physics.[10]

A major objective is to understand the properties of matter at high pressure and density, and shock compression is a widely used experimental technique for this. For details see reference 10 and references therein. The Rankine-Hugoniot equations relate the initial pre-shocked values to the final shocked values through shock and particle velocities. The final shocked state can be determined from the initial state if these two velocities can be measured. For pressures less than a few Mbar, high explosives or gas guns are used to accelerate fliers. Between 10 and 10^4 Mbar there are different theoretical predictions for the principal Hugoniot (the pressure-density curve for a singly shocked material), and oscillations are predicted from pressure ionization. The NIF should be able to access these pressures, thus addressing the uncertainties in current understanding. Shocks are produced in packages mounted to hohlraum walls, driven by the hohlraum-produced x-rays. Shaping the laser intensity in time allows either a single shock (principle Hugoniot) or a series of shocks (almost adiabatic compression) to be studied. The shock velocity can be measured by the shock break-out (PSBO and ASBO) or VISAR diagnostics. The particle velocity is measured using x-ray side-lighting: careful choice of a pusher or piston material that is opaque and a sample that is transparent allows the piston-sample boundary to be seen in transmission by a streaked x-ray imager. Side lighting also provides the shock velocity by refraction of the x-rays at the steep density gradient associated with the shock.

Hydrodynamic instabilities and material mixing in radiation fields occur in nuclear weapons, supernova explosions, and ICF implosions. Again details are found in reference 10 and references therein. The radiation field is important because it modifies density gradients and introduces mass ablation, both of which affect growth. The main instabilities are Rayleigh-Tayor, Richtmeyer-Meshov, and Kelvin-Helmholtz. Experimental techniques use shock tubes (a few bars, compression, no radiation), high explosives (300 kBar, low compression, no radiation), gas guns (Mbars, modest compression, no radiation) and fluid-cell accelerators (incompressible, no radiation). On the NIF acceleration of 10^{14}g will be available, with pressures >100 Mbar, and high radiation. Surfaces can be prepared with known perturbations, and driven by hohlraum x-ray radiation. Face-on x-ray back-lighting (radiography) is one experimental technique.

Radiation physics experiments include opacity measurements, performed on uniformly x-ray heated samples in local thermal dynamic equilibrium. The opacity is measured by point projection absorption spectroscopy. Critical high-z opacity measurements should be possible with the hotter hohlraums available on the NIF (smaller than those used for ignition).

5   Radiation effects physics

The radiation effects experiments on the NIF are initially devoted to developing x-ray sources that can simulate threat environments.[1] Laser-produced plasmas are efficient sources of x-rays. For the NIF, kilojoules to megajoules of x-rays can be generated from a millimeter-size source, depending on the energy of interest. Radiation sources driven on flat targets can be configured as point sources, with increased spatial coherence, or as large-area radiators for efficient radiative energy transfer in a close-coupled geometry. The most intense radiation environment created using a high-energy laser is found inside a hohlraum. Continuum x-ray sources, conveniently described by effective blackbody temperatures, can easily be spectrally filtered and tailored. At the highest energies, implosion experiments on the NIF will achieve capsule temperatures of 5-10 keV, which will produce extremely bright bursts of continuum, hard x-rays. Short-pulse capability on the NIF will allow the generation of intense, hard x-ray sources in the ultra short temporal regime, allowing study of the dynamics of materials undergoing rapid phase transformations on the time scale of individual atomic motion. Line sources can yield narrow-bandwidth radiation with increased temporal coherence. They represent an important diagnostic tool for hard x-ray imaging and opacity measurements, in addition to their use as effects sources. Conversion efficiency into a single spectral line has been measured to vary from 1% at x-ray energies below 3 to 4 keV to 0.1% above 4 keV. The character of the emission spectra is strongly affected by the dominant shell. For instance, K-shell emitters are dominated by isolated strong hydrogen-like and helium-like line emission. In contrast, high-Z emitters such as gold are dominated by large bands of unresolved transitions. The NIF laser will allow higher ionization states to be accessed, extending the region of monochromatic x-ray sources to the hard x-ray region.

A 1 to 10 keV point source with low debris and good spectral fidelity will be developed using low-z material hohlraums filled with gas (e.g. Xe) and irradiated by ~40 TW. A distributed source can then be produced using multiple single point sources as indicated in Figure 8. Laser beam steering is an important consideration. Higher energy sources (up to 30 keV), both thermal (hohlraum) and Bremmstrahlung, will then be developed, and used for testing.
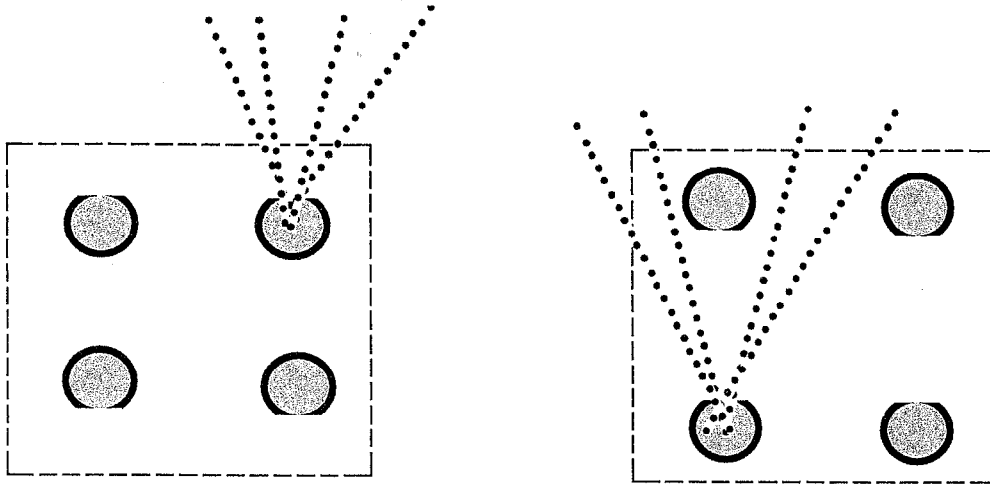
Fig. 8: Two possible irradiation geometries in which point sources are combined to approximate a distributed source. The broken lines indicate the laser beam geometry entering the individual source hohlraums.

6 Basic science and inertial fusion energy physics

First concerning inertial fusion energy (IFE), recent progress in target physics and target design for high energy gain in the U.S. inertial fusion research programs supports the possibility of developing an attractive fusion power plant, using either laser or heavy ion drivers. Success of the NIF ignition program, expected within the next decade, together with advanced numerical models, will provide confidence that the gains needed in future IFE plants can be achieved.[9] Based on these expected target gains, IFE power plant studies show the promise of an acceptable cost of electricity and environmentally attractive plant designs for both heavy-ion and laser-driven IFE. The major research issues for IFE are dominantly technological, rather than the achievement of ignition itself. These issues include the development of a driver, target production, and repetition rate; all within a reasonable budget. Details are found in reference 11 and references therein.

NIF fuel capsules are designed to absorb 0.1 to 0.2 MJ of x-rays while capsules envisioned for energy production typically absorb 1 to 2 MJ of x rays. However after ignition occurs, the burn wave propagates in ρr and temperature space in a way that is essentially independent of size. Thus information for NIF capsules is widely applicable to capsules with larger yield, and can be used to design the higher yield capsules generally appropriate for energy production. If warranted by results of current research, the NIF could be modified to test fast ignition as well.

Table 1. Possible categories of basic science experiments suitable for study on the NIF.

Hydro-dynamics	Material Properties	Radiative properties	Radiation Sources	Plasma Physics
1. Stable Flow	1. The Principal Hugoniot/EOS	1. Spectroscopy at High-Z	1. Incoherent x-ray Sources	1. Laser-Plasma Interactions
a) Shock-Shock Interactions	2. Multiple Shock States	2. Transparency Window	*a) Broadband Sources*	*a) Long Scale-Length Plasmas*
b) Shock Boundary Interactions	3. Isentropic Release States	3. Strongly Correlated Effects	*b) Narrow or Line Sources*	*b) SBS and SRS*
c) Hypersonic Flow	4. Isochoric Heating	4. Plasma Spectroscopy	2. Coherent x-ray Sources	*c) Filamentation*
d) Impact Cratering	5. X-ray Diffraction	5. Population Kinetics	*a) High-Order Harmonic Generation*	1. Short-Pulse High-Intensity Laser-Plasma
e) Radiative Energy Coupling	6. Other Material Properties (diffusivities..)	2. Radiation Transfer and Line Formation	*b) Applications of x-ray Lasers*	3. Very High Magnetic Fields
2. Unstable Flow	7. Opacity	4. Strong Magnetic Field Effects	*c) Particle Sources*	3. High Flux , Energy Electrons
d) Classical Instabilities	8. Material strength		3. Applications of laser based x-ray sources	4. Interpenetrating Plasmas and Turbulence
e) Other Instabilities				5. Nuclear Reactions
f) Turbulent Flow, Vortex				6. Plasma Streaming in B Fields

Turning to basic science, there are many areas in which the NIF can contribute.[12] Table 1 summarizes the topics under the main headings of hydrodynamics, material properties, radiative properties, radiation sources and plasma physics. As an example consider the spectroscopy of high-Z elements. Using the NIF laser with special foam target designs, or using other mechanisms for producing long-scale-length plasmas, coronal temperatures of 6 keV or even 10-keV can be produced. This will make it possible to probe most elements of the periodic table to any desired degree of ionization. While other sources of high-Z ions (e.g. EBIT and Tokamak) exist, they do not efficiently excite the transitions between excited states. Thus, the NIF will allow the study of entire spectra of highly charged ions that cannot be produced by currently available lasers.

7 Conclusions

The NIF represents the first of a new generation of lasers with megajoule energy in the few eV photon energy range. Its major purpose is to address stockpile stewardship issues of high-energy-density physics, including measurements of equation of state, studying hydrodynamic instabilities, and opacity. A major campaign will be that of ignition and propagating burn. It will provide x-ray sources for radiation testing. At the same time it will contribute to basic science and inertial fusion energy research. First light is expected in 2002, and the indirect x-ray drive ignition campaign will start in 2007.

References

1. Facilities User Plan of the National Ignition facility, editors Hauer, Kauffman, Satsangi, Haill, Cauble and Saito, report LALP-97-7, UC-700 (1997).
2. Energy and Technology Review, UCRL-52000-94-12 (December 1994).
3. http://www.sandia.gov/ASCI/
4. National Technical Information Service Document numbers DE 95107671 through DE 95017673 and DE 95017676 through DE 95017700 (J. A. Paisner, E. M. Campbell and W. J. Hogan, The National Ignition Facility Project, UCRL-JC-117397 and UCRL-PROP-117093 (1994)).
5. J. A. Paisner, E. M. Campbell and W. J. Hogan, Fusion Technology 26 755 (1994).
6. J. Hunt, K. Manes, J. Murray, P. Renard, R. Sawicki, J. Trenholme and W. Williams, Fusion Technology 26 755 (1994)
7. J. Lindl. Phys. Plasmas 2 3933 (1955)
8. R. J. Leaper et al., Rev. Sci. Instrum. 68 868 (1997)
9. J. D. Kilkenny et al, Phil. Trans. R. Soc. Lond. A 357 533 (1999).
10. E. M. Campbell, N. Holmes, S. Liby, B. Remington and E. Teller, Lasers and Particle Beams 15 1 (1997).
11. Energy from Inertial Fusion, IAEA Vienna (1995).
12. http://www.llnl.gov/science_on_lasers/DocMap.html#Map